Indian Journal of Science and Technology, *Vol 9(28), DOI: 10.17485/ijst/2016/v9i28/97775, June 2016*
ISSN (Print) : 0974-6846
ISSN (Online) : 0974-5645

Pristine Study of Axial Tensile Strain Energy Curve for Single-Walled Carbon Nanotube using Molecular Dynamics Simulation

Ai-Ping Tan[1]*, Su-Hoe Yeak[1] and Riadh Sahnoun[2]

[1]Department of Mathematical Sciences, Faculty of Science, UniversitiTeknologi Malaysia, 81310 Skudai, Johor, Malaysia; aptan317@hotmail.com

[2]Center for Sustainable Nanomaterials, IbnuSina Institute for Fundamental and Industrial Research, Universiti Teknologi Malaysia, 81310 Skudai, Johor, Malaysia

Abstract

Although the discovery of carbon nanotube was dated back in 1952 by Radushkevich and Lukyanovich, it has attracted attention of the industrial and scientific communities only when Iijima succeeded in synthesizing the first Multi-Walled Carbon Nanotubes (MWCNTs) in 1991. The unique properties of carbon nanotubes, in particular mechanical, have sparked designing, fabrication and commercialization of robust carbon nanotube based materials. The robustness of any material, i.e., the mechanical properties, is in factgreatly affected by the presence of defects. In this paper, one of the mechanical properties for the zigzag type Single Walled Carbon Nanotubes (SWCNTs) is studied. The strain energy curve under axial tensile loads is determined by using the Molecular Dynamics (MD) simulation. The interaction force between atoms is modeled by using the second-generation of Reactive Empirical Bond-Order (REBO) potential coupled with the Lennard-Jones potential. The validation with Young's modulus is presented and discussed. The effect of the size of the tube diameter of SWCNT on the strain energy curve is also discussed.

Keywords: Axial Tensile Strain, Molecular Dynamics, Strain Energy, Young's Modulus, Zigzag Type Carbon Nanotubes

1. Introduction

The first discovery of Carbon Nanotubes (CNTs) shall be credited to Radushkevich and Lukyanovich in the year 1952, where they published the transmission electron microscopy evidence for tubular nature of some nano-sized carbon filament with diameters of carbon nanotube reaching up to 50 nanometers[1]. However, the scientist who boosted carbon nanotubes to receive particular interest from industrial and scientific communities[1,2] was[3], who succeeded to synthesize Multi-Walled Carbon Nanotubes (MWCNTs) in 1991. The tremendous interest in CNTs is reflected by the availabilityof commercial carbon nanotube based materials which appeared right after the discovery of the properties of the Single-Walled Carbon Nanotubes (SWCNTs). SWCNTs were first discovered in 1993 by two independent research groups[4,5]. Many researchers have used Single-Walled Carbon Nanotubes (SWCNTs) as the model systems in their works[6]. Numerous theoretical and experimental studies have been carried out to understand and further improved the SWCNTs impressive properties such as mechanical properties[2,7].One way to unveil the ambiguous in SWCNTs marvelous mechanical properties was the calculation of the strain energy of these materials[8]. Based on the details obtained from the properties, numerous devices have been designed using CNTs[9,10].

There are two kinds of distortion for SWCNTs in studying the strain energy curve, which are under axial compression and under axial tension. Unlike axial tension, much attention has been paid to axial compression[11]. Furthermore, there is necessity to investigate the connection between the diameter of the CNT and its strength (robustness) limit since the strength of materials is greatly affected by the presence of defects. So far, only several

*Author for correspondence

research works have been reported in the literature and for which the relationship between the strain energy with the diameter of the SWCNTs (in particular the zig-zag type) has been studied[12]. Therefore, in this paper, our attention will be particularly paid to investigate the strain energy curve of zigzag SWCNTs for four different diameters under tensile loads by using Molecular Dynamics (MD) simulation.

2. Fundamental Parameters Description for Zigzag SWCNTs

Initially, the electronic structure of zigzag type SWCNT is generated with coordinates of each carbon atom. Consider the basis vectors $\mathbf{a}_1$ and $\mathbf{a}_2$ of the hexagon lattice and a nomenclature (n,m) which refers to integer indices for the basis vectors, the chiral vector $\mathbf{C}_h$ can be used to specify SWCNT. For zigzag type, m is always equal to zero. Table 1 clearly shows the relationship for the parameters in brief.

The first column represents the symbols for parameters used in constructing zigzag SWCNT. Figure 1 elucidates

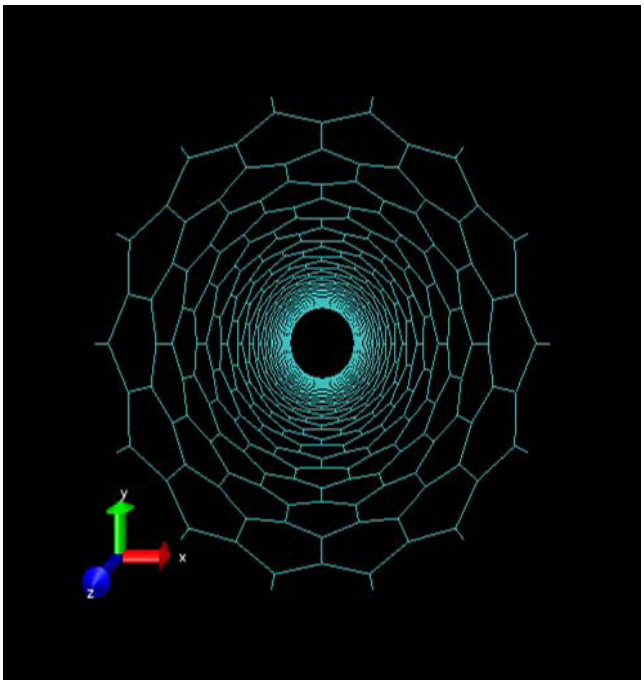

Figure 1. (14,0) zigzag SWCNT visualized using software VMD version 1.8.7[14].

Table 1. Description of parameters[13] for Zigzag SWCNT

Symbol	Name	Formula
$a_{c\text{-}c}$ [=1.42Å]	Carbon-carbon distance	
a [=2.46Å]	Length of unit vectors	$3^{1/2}a_{c\text{-}c}$
$\hat{\mathbf{a}}_1, \hat{\mathbf{a}}_2$	Unit vectors	$(3^{1/2}/2, 1/2)a$, $(3^{1/2}/2, -1/2)a$
$\hat{\mathbf{e}}_1, \hat{\mathbf{e}}_2$	Reciprocal lattice vectors	$(1/3^{1/2}, 1)2\pi/a$, $(1/3^{1/2}, -1)2\pi/a$
$\hat{\mathbf{C}}_h[=n\hat{\mathbf{a}}_1]$	Chiral vector	$\hat{\mathbf{C}}_h = n\hat{\mathbf{a}}_1 + m\hat{\mathbf{a}}_2 = (n,m)$
C [=an]	Circumference of SWCNT	$C = \lvert\hat{\mathbf{C}}_h\rvert = a\,(n^2+m^2+nm)^{1/2}$
D [=na/π]	Diameter of SWCNT	$D = C/\pi = [a\,(n^2+m^2+nm)^{1/2}]/\pi$
Θ [=0]	Chiral angle	$\cos\theta = (2n+m)/[2(n^2+m^2+nm)^{1/2}]$
d [=n]	The highest common divisor of (n, m)	
d_R [=n]	The highest common divisor of (2n+m, 2m+n)	If (n-m) not a multiple of 3d: d_R=d If (n-m) is a multiple of 3d: d_R=3d
$\check{\mathbf{T}}$ [=(1,-2)]	Translational vector of 1D unit cell	$\check{\mathbf{T}} = t_1\hat{\mathbf{a}}_1 + t_2\hat{\mathbf{a}}\mathbf{2} = (t_1, t_2)$ $t_1 = (2m+n)/d_R$; $t_2 = -(2n+m)/d_R$
T [=$3^{1/2}$a]	Length of $\check{\mathbf{T}}$	$T = (3^{1/2}C)/d_R$
N [=2n]	Number of hexagons per 1D unit cell	$N = [2(n^2+m^2+nm)]/d_R$
$\hat{\mathbf{R}}$	Symmetry vector	$\hat{\mathbf{R}} = p\hat{\mathbf{a}}_1 + q\hat{\mathbf{a}}\mathbf{2} = (p, q)$
R	Basic symmetry operation	$R = (\Psi\lvert\tau)$
M [=1]	Number of 2π revolutions	$M = [(2n+m)p+(2m+n)q]/d_R$ $N\hat{\mathbf{R}} = M\hat{\mathbf{C}}_h + d\check{\mathbf{T}}$
Ψ [=π/n]	Rotation operation	$\Psi = (2\pi M)/N$, $[\chi = (\Psi C)/(2\pi)]$
τ [=($3^{1/2}$a)/2]	Translation operation	$\tau = (d\check{\mathbf{T}})/N$

the schematic structure for (14,0) zigzag SWCNT. Further details for the parameters can be found in the work reported by Dresselhaus and co-workers[13].

3. Molecular Dynamics Simulation

After forming the SWNTs, microcanonical ensemble MD simulation is performed by using the classical MD method to compute the interaction force between atoms in a system with time step of 1 femtosecond. The integration method used in MD is the Gear's predictor-corrector algorithm[15].

Generally, the force is derived from the gradient of energy or force field. The force field is equal to the summation of short range potential and long range van der Waals potential. Here, the short range interatomic force is modeled by second generation of Reactive Empirical Bond Order (REBO) potential[16] where the long range interatomic force is modeled using Lennard-Jones (LJ) 12-6 potential[17]. Given that the indices (i,j) represent the counting number for two bonding atoms, the potential is given by

$$E = \sum_{i} \sum_{j>i} \left(E_{ij}^{REBO} + E^{vdW} \right). \quad (1)$$

The REBO potential considers the whole system as bonding interaction, where only nearest-neighbors of carbon-carbon covalent bond contribute to the energy in the system. The bonding interaction is classified into two main pair interactions, which are repulsive V_R and attractive V_A pair interactions. The REBO potential can be simplified as

$$E_{ij}^{REBO} = \left[V_R(r_j) + b_j V_A(r_j) \right], \quad (2)$$

Where b_{ij} is the bond order and r_{ij} is the interatomic distance between atom i and j. The repulsive and attractive interactions are defined as

$$V_R(r_j) = f^c(r_j) \left(1 + \frac{Q}{r_j} \right) A e^{-\alpha r_{ij}}, \quad (3)$$

$$V_A(r_j) = f^c(r_j) \sum_{n=1,3} B_n e^{-\beta_n r_j}, \quad (4)$$

where the first term is a function of interatomic distance that acted as the control function, so that only the interatomic distance in the range between 1.7 until 2.0 Å are accepted as the nearest-neighbor atoms. Parameters such as Q, A, α, B_n and β_n listed in Table 2 are the adjusting fitting parameters corresponding to dataset. The better description for parameters can be referred to the work by Brenner and his co-workers[16].

It should be noted that Lennard-Jones 12-6 potential[17] will be included in the computation only if the covalent potential is found equal to zero. Typically, Lennard-Jones 12-6 potential is written as

$$E^{II} = 4\varepsilon \left[\left(\frac{\sigma}{r_j} \right)^{12} - \left(\frac{\sigma}{r_j} \right)^{6} \right], \quad (5)$$

where the ε is the depth of potential well, σ is the finite separation of distance at which the bonding potential energy is zero[18].

4. Results and Discussion

4.1 Axial Tensile Strain, Stress and Young's Modulus

Forces are applied at the both ends of the SWCNT, as shown in Figure 2.

Given that T is the current length of SWCNT at certain time, and T_0 is the initial length of SWCNT, the axial tensile strain is written as

$$\delta = \frac{\Delta T}{T_0} = \frac{T - T_0}{T_0}. \quad (6)$$

By summing the interatomic forces for atoms at the ends of SWCNT, the axial force can be calculated. Stress

Table 2. Adjusting parameters for Equation (3) and (4).

List for fitting parameters[16]		
B_1 = 12388.79197798eV	β_1 = 4.7204523127Å^{-1}	A = 10953.544162170eV
B_2 = 17.56740646509eV	β_2 = 1..4332132499Å^{-1}	α = 4.7465390606595Å^{-1}
B_3 = 30.71493208065eV	β_3 = 1.3826912506Å^{-1}	Q = 0.3134602960833Å

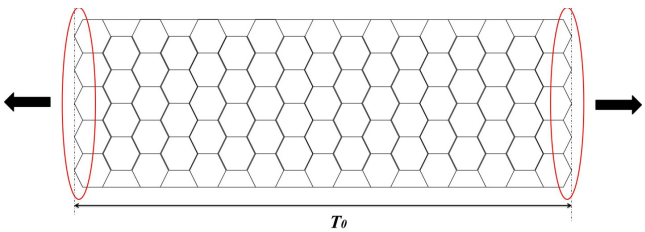

Figure 2. Two-dimensional view for the SWCNT under axial tension.

is equal to the axial force over the cross-sectional area, where the cross-sectional area is πhD, where h is thickness of the SWCNT, and D is the tube diameter of the SWCNT. Here, the thickness is fixed, and is equal to 3.4 Å. Young's modulus can be obtained from the ratio of stress to axial tensile strain. In order to validate the MD coding, Young's modulus is calculated and compared with those reported in the literature (Table 3).

Our Young's moduli for two small size of zigzag SWCNTs which contained 840 atoms and 1360 atoms were computed andcompare reasonably well with those reported in the literature[19] evidencing the reliability of our coding. Although the same size of total atoms and same potential are adopted, the slightly deviation in Young's moduli may be attributed to the adjusting parameters involved in MD method. Moreover, the SWCNT structural parameters such as tube length and tube diameter may also be sensitive to the calculation.

4.2 Strain Energy

Strain energy computed from this work is equal to the difference between the current energy with the initial energy. Strain energy proposed by[20] is given as

$$E = \frac{\pi h^3 \mathbf{Y}}{6D}, \qquad (7)$$

where Y is the Young's modulus, T is the tube length, h is thethickness of the SWCNT and D is the tube diameter of the SWCNT. By substituting the Young's modulus in terms of strain energy, the equation can be simplified as

$$E = \frac{\pi h^3}{6}\frac{T}{D}\frac{1}{\pi hDT}\frac{\partial^2 E}{\partial \delta^2} = \frac{h^2}{6}\frac{1}{D^2}\frac{\partial^2 E}{\partial \delta^2}. \qquad (8)$$

From Equation (8), it is clearly shown that the axial tensile strain and tube diameter contribute to the strain energy, given that the axial tensile strain is the changing ratio for the tube length. Therefore, tube length and tube diameter are both affecting factors to the strain energy. To identify which of the two affecting parameters is more significant to the strain energy, we have varied the size of the zigzag SWCNT (the index n) from four to seven. Here, the starting structure was 160 carbon atoms to which added systematically and consistently 40 carbon atoms until reaching 280 carbon atoms. Details of the-structures for four zigzag SWCNTs are listed in Table 4 and 5. It is clear from these tables that the tube diameters of the zigzag SWCNT are changing consistently while the tube lengths are not.

Assuming that there is relationship between the strain energy with thetube diameter of the SWCNT, then the change in the strain energy curve versus axial tensile strain should be quite reasonable. Figure 3 illustrates the strain energy curve against axial tensile strain for four different type of zigzag SWCNTs. One can see that the obvious fluctuations of the curves started at axial tensile strain near 0.16, and for index equal to 7, the fluctuation starts at 0.14. This means that the materials start to deform once the elastic limit is achieved.

Table 3. Comparison of Young's modulus

Index, (n,m)	Total atom, Ξ	Tube length, T (Å)	Tube diameter, D (Å)	Young's modulus, Y (GPa)	Source
(14,0)	840	62.30	10.96	939.032	Work in [19]
		62.41	10.97	929.903	Present work
(17,0)	1360	83.62	13.30	938.553	Work in [19]
		83.73	13.32	912.641	Present work

Table 4. Structural parameters and Young's modulus for the studied zigzag SWCNTs

Index, (n,m)	Total atom, Ξ	Tube length, T (Å)	Tube diameter, D (Å)	Young's modulus, Y (GPa)
(4,0)	160	40.30	3.13	807.960
(5,0)	200	40.66	3.92	832.419
(6,0)	240	40.84	4.70	845.174
(7,0)	280	40.94	5.48	854.290

Table 5. Variation of ΔT, ΔD, and ΔY with increasing the size of the SWCNT

System change	$\Delta\Xi^{(a)}$	$\Delta T^{(b)}$ (Å)	$\Delta D^{(c)}$ (Å)	$\Delta Y^{(d)}$ (GPa)
(4,0)→(5,0)	40	0.36	0.78	24.459
(5,0) →(6,0)	40	0.18	0.78	12.755
(6,0) →(7,0)	40	0.10	0.78	9.116

Descriptions:
$\Delta\Xi^{(a)}$ is the difference total atom between consecutive zigzag SWCNT.
$\Delta T^{(b)}$ is the difference tube length between consecutive zigzag SWCNT.
$\Delta D^{(c)}$ is the difference tubediameter between consecutive zigzag SWCNT.
$\Delta Y^{(d)}$ is the difference Young's Modulus between consecutive zigzag SWCNT.

Before reaching the fluctuation region, it can be seen from Figure 3 that the deviation between the curves is showing consistent changing with increasing the number of carbon atoms. This is a clear evidence to show that the tube diameter of the zigzag SWCNT might play a significant role in contributing to the strain energy at this region, since it is the only parameter showing consistency. The strain energy curves before the material undergoes deformation will be further investigated, as will be seen later. Considering that the tube diameter is the main consistent parameter and the tube length slightly contributes to the strain energy, the strain energy curves before the fluctuation region should be foreseen in the next few systems in which the strain energy curve can be predicted systematically. Therefore, the curve fitting process with polynomial of degree two has been evaluated for four different zigzag types, so that it can capture our assumption. The adjusting parameters are gathered in Table 6. The strain energy can be reproduced using the fitting parameters and the axial tensile strain. The fitting function is written as

$$E = c_1\delta^0 + c_2\delta^1 + c_3\delta^2. \quad (9)$$

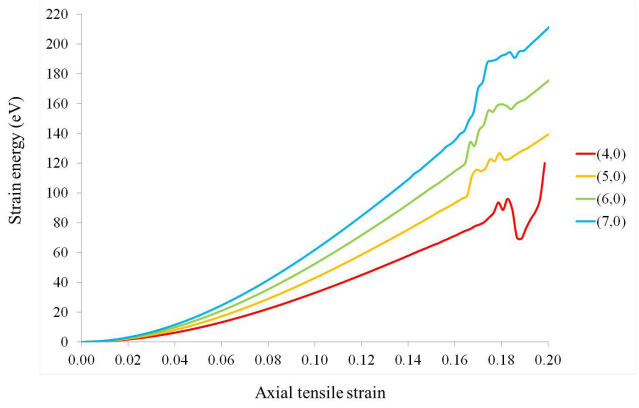

Figure 3. Comparison between strain energy curves of zigzag SWCNTs for (4,0), (5,0), (6,0) and (7,0) under axial tensile.

Table 6. Fitting parameters for strain energy curves against 14% axial tensile strain

Index, (n,m)	Coefficients		
	c_1	c_2	c_3
(4,0)	-1.09	99.96	2347.44
(5,0)	-1.40	128.72	3070.76
(6,0)	-1.68	153.89	3787.78
(7,0)	-1.96	177.33	4504.19

To determine the predicted coefficients of the polynomial for (6,0) system for example, two ways can be proposed and give similar results. In fact, the predicted coefficients for (6,0) is

$$c_1 = 2(-1.\theta) - (-1.\theta) = (-1.\theta) + [(-1.\theta) - (-1.\theta)] = -1.7 \ . \quad (10)$$

It is clear that the fitting parameters have a simple relationship. By using this relationship and converting it into the relationship for strain energy $E = 2E_{-1} - E_{-2}$, the strain energy curve for (6,0),(7,0), (8,0), (9,0), (10,0), and (11,0) can be estimated as shown in Table 7. With these predicting parameters, the strain energy curve can be reasonably estimated.

Figure 4 illustrates the strain energy curves with the predicted strain energies. The line curves represent the data collection of strain energies from MD method. The cross signs represent the computed strain energy by using the predicted parameters. These predicted fitting curves (extrapolated points) for then justify our assumptions.

Table 7. Parameters predicted from fitting parameters

Index, (n,m)	Coefficients		
	c_1	c_2	c_3
(6,0)	-1.71	157.48	3794.08
(7,0)	-1.96	179.06	4504.80
(8,0)	-2.24	200.77	5220.60
(9,0)	-2.52	222.49	5921.57
(10,0)	-2.80	244.29	6616.44
(11,0)	-3.04	265.06	7312.50

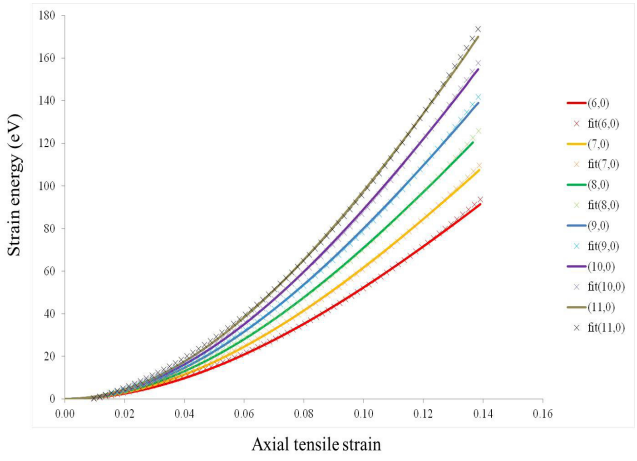

Figure 4. Curve fitting strain energy curves by using predicting parameters.

5. Conclusions

In this paper, the MD simulation for zigzag type under axial tensile was carried out. The calculated Young's moduli for SWCNTs compare reasonably well with those reported in the literature, validating and evidencing the reliability of our coding. Although the same size of total atoms and same potential are adopted, slightly different Young's moduli were found which can be attributed to the adjusting parameters involved in MD method, in addition to the fact that the SWCNT structures constructed may also be sensitive to the calculation. From the simulations, the strain energy curves which elaborate the elastic behaviors are obtained. The strain energy curves clearly show consistent increment in deviation between curves before 0.14 axial tensile strains, suggesting that the diameter is a significant affecting parameter for strain energy in this region. We further explored the possibility of predicting the parameters of the strain energy for larger SWCNTs. The proposed equation gave reasonable strain energy.

6. Acknowledgements

The financial supports from Ministry of Higher Education Malaysia (MOHE) through MyBrain15 scholarship (MyPhD), and from Universiti Teknologi Malaysia (UTM) through Fundamental Research Grant Scheme (FRGS) R.J.130000.7826.4F622 are fully acknowledged.

7. References

1. Monthioux M, Kuznetsov VL. Who should be given the credit for the discovery of carbon nanotubes? Carbon. 2006 Aug; 44(9):1621–3.
2. Terrones M. Science and technology of the 21st century: Synthesis, properties, and applications of carbon nanotubes. Annu Rev Mater Res. 2003 Aug; 33:419–501.
3. Iijima S. Helical microtubules of graphitic carbon. Nature. 1991 Nov; 354:56–8.
4. Iijima S, Ichihashi T. Single-shell carbon nanotubes of 1-nm diameter. Nature. 1993 June; 363:603–5.
5. Bethune DS, Kiang CH, Devries MS, Gorman G, Savoy R, Vazquez J, Beyers R. Cobalt-catalysed growth of carbon nanotubes with single-atomic-layer walls. Nature. 1993 Jun; 363:605–7.
6. Kiang CH, Goddard III WA, Beyers R, Bethune DS. Carbon nanotubes with single-layer walls. Carbon. 1995 Feb; 33(7):903–14.
7. Iijima S. Carbon nanotubes: Past, present, and future. Physica B. 2002 Oct; 323:1–5.
8. Zhou X, Zhou JJ, Ou-Yang ZC. The strain energy and Young's modulus of single-wall carbon nanotubes calculated from the electronic energy-band theory. Phys Rev B. 2000 Nov; 62:13692–6.
9. Srivastava D, Wei CY, Cho KJ. Nanomechanics of carbon nanotubes and composites. Appl Mech Rev. 2003 Mar; 56(2):215–30.
10. De Volder MFL, Tawfick SH, Baughman RH, John Hart A. Carbon nanotubes: Present and future commercial applications. Science. 2013 Feb; 339:535–9.
11. Liew KM, He XQ, Wong CH. On the study of elastic and plastic properties of multi-walled carbon nanotubes under axial tension using molecular dynamics simulation. Acta Mater. 2004 May; 52:2521–7.
12. Rubaiyat SNH, Chowdhury SC. Study of pristine carbon nanotube under tensile and compressive loads using molecular dynamics simulation. Journal of Mechanical Engineering. 2009 Dec; 40(2):72–8.
13. Dresselhaus MS, Dresselhaus G, Saito R. Physics of carbon nanotubes. Carbon. 1995; 33(7):883–91.
14. Humphrey W, Dalke A, Schulten K. VMD– Visual Molecular Dynamics. J Molec Graphics. 1996; 14(1):33–8.
15. Gear CW. Numerical initial value problem in ordinary differential equations. NJ, USA: Prentice-Hall PTR; 1997.
16. Brenner DW, Shenderova OA, Harrison JA, Stuart SJ, Ni B, Sinnott SB. A second-generation Reactive Empirical Bond Order (REBO) potential energy expression for hydrocarbons. J Phys – Condens Mat. 2002 Jan; 14:783–802.
17. Jones JE. On the determination of molecular fields. I. From the variation of the viscosity of a gas with temperature. P. R Soc Lond A-Conta. 1924 Oct; 106(738):441–62.
18. Israelachvili JN. Intermolecular and surface forces. 3rd ed. San Diego: Academic Press; 2011.
19. Bao WX, Zhu CC, Cui WZ. Simulation of Young's modulus of single-walled carbon nanotubes by molecular dynamics. Physica B. 2004 Oct; 352:156–63.
20. Tibbetts GG. Why are carbon filaments tubular? J Cryst Growth. 1984; 66:632–8.